The EMBO Journal vol.14 no.5 pp.918–926, 1995

Mitotic HeLa cells contain a CENP-E-associated minus end-directed microtubule motor

Douglas A.Thrower[1,4], Mary Ann Jordan[1], Bruce T.Schaar[2,3], Tim J.Yen[2] and Leslie Wilson[1]

[1]Division of Molecular, Cellular, and Developmental Biology, Department of Biological Sciences, University of California, Santa Barbara, CA 93106, [2]Institute for Cancer Research, Fox Chase Cancer Center, 7701 Burholme Avenue, Philadelphia, PA 19111 and [3]Cell Biology Graduate Group, University of Pennsylvania, Philadelphia, PA 19104, USA

[4]Corresponding author

Communicated by M.Osborn

A minus end-directed microtubule motor activity from extracts of HeLa cells blocked at prometaphase/metaphase of mitosis with vinblastine has been partially purified and characterized. The motor activity was eliminated by immunodepletion of Centromere binding protein E (CENP-E). The CENP-E-associated motor activity, which was not detectable in interphase cells, moved microtubules at mean rates of 0.46 μm/s at 37°C and 0.24 μm/s at 25°C. The motor activity co-purified with CENP-E through several purification procedures. Motor activity was clearly not due to dynein or to kinesin. The microtubule gliding rates of the CENP-E-associated motor were different from those of dynein and kinesin. In addition, the pattern of nucleotide substrate utilization by the CENP-E-associated motor and the sensitivity to inhibitors were different from those of dynein and kinesin. The CENP-E-associated motor had an apparent native molecular weight of 874 000 Da and estimated dimensions of 2 nm × 80 nm. This is the first demonstration of motor activity associated with CENP-E, strongly supporting the hypothesis that CENP-E may act as a minus end-directed microtubule motor during mitosis.

Key words: CENP-E/dynein/kinesin/microtubule motor/mitosis

Introduction

Centromere binding protein E (CENP-E), initially identified using a monoclonal antibody (177) raised against fractionated chromosomal proteins (Yen *et al.*,1991), is a 312 kDa protein that belongs to the kinesin superfamily (Yen *et al.*, 1992). The N-terminal region of CENP-E shares strong sequence homology with the microtubule motor domain of kinesin and kinesin-like proteins (KLPs) (Goldstein, 1993) and binds to microtubules in an ATP-sensitive manner (Liao *et al.*, 1994). Thus it has been suggested that CENP-E, like kinesin, may be a microtubule motor.

CENP-E is present in the cytoplasm of HeLa cells at very low levels during G_1 or early S phase and its expression increases during late S phase and G_2, reaching a peak at the transition between G_2 and mitosis (Brown *et al.*, 1994). By immunofluorescence microscopy with a monoclonal antibody specific for CENP-E (antibody 177), CENP-E was found to localize initially at the kinetochores of chromosomes during early prometaphase of mitosis. It remains at kinetochores until anaphase, when it becomes redistributed to the spindle midzone. It then becomes localized in the midbody at the end of mitosis (Yen *et al.*, 1991) and appears to be degraded following anaphase (Brown *et al.*, 1994). CENP-E appears to play a role in chromosome movement during mitosis (Yen *et al.*, 1992). For example, injection of antibody 177 into cells during prometaphase delays or prevents progression from metaphase to anaphase (Yen *et al.*, 1991).

In the present work, we describe the properties of a motor activity that is enriched in extracts from HeLa cells blocked in prometaphase/metaphase with 2–5 nM vinblastine. The motor moves along microtubules towards the minus ends of microtubules and the motor activity is depleted from HeLa extracts by an antibody specific for CENP-E. CENP-E co-purifies with the motor activity during a microtubule-affinity purification step and by sucrose density gradient fractionation, suggesting that the motor activity may be due to CENP-E.

Results

Extracts of mitotic HeLa cells contain a microtubule motor activity that is not detectable in interphase cell extracts

We unexpectedly detected microtubule motor activity in supernatants of centrifuged lysates of mitotic HeLa cells (S-100 extracts, Materials and methods) while analyzing the effects of the extracts on dynamic instability behavior of microtubules *in vitro*. The activity was barely detectable in the extracts because a significant proportion of the microtubules was immobilized by association with large membrane-like structures similar to those observed in *Xenopus* egg extracts (Allan and Vale, 1991). Fractionation of the mitotic S-100 extracts by DEAE–cellulose column chromatography yielded a fraction (D-100, Materials and methods) which did not contain microtubule-associated membranous networks. When taxol-stabilized bovine brain microtubules were added to the D-100 mitotic fractions on coverslips in the presence of 1 mM ATP and examined by video microscopy, >90% of the microtubules exhibited gliding behavior. The microtubules glided continuously in a directional manner indicating that the gliding was caused by a microtubule motor.

The motor activity in D-100 fractions from mitotic extracts moved microtubules in the presence of 1 mM ATP at mean rates of 0.46 ± 0.03 μm/s at 37°C (Figure 1) and 0.24 ± 0.02 μm/s at 25°C (data not shown). The rate

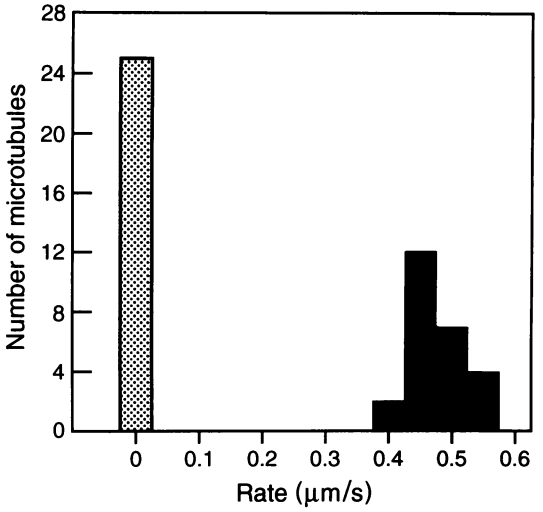

Fig. 1. Microtubule gliding supported by mitotic but not interphase HeLa cell extracts. HeLa mitotic D-100 fractions (solid bars) (8 mg/ml total protein) or D-100 fractions of interphase cells (stippled bar) (8 mg/ml total protein) were incubated on coverslips for 15 s. Solutions of taxol-polymerized bovine brain microtubules in 1 mM ATP were then added. The mean (standard deviation) rate of movement of 25 microtubules in mitotic extracts at 37°C was 0.46 ± 0.03 μm/s. No movement could be detected with 25 microtubules in D-100 interphase extracts.

of microtubule movement did not increase when the D-100 fractions were concentrated 4-fold or when the ATP concentration was increased to 10 mM. The motor activity is ~4-fold slower than that of HeLa cell dynein (described below) and is slower than that of kinesin (0.4–0.9 μm/s at 22–25°C, Vale *et al.*, 1985; Porter *et al.*, 1987; Saxton *et al.*, 1988). D-100 fractions of interphase cells prepared in a manner identical to D-100 fractions of mitotic cells had no detectable microtubule motor activity (Figure 1).

The D-100 mitotic motor is minus end-directed

The direction of the HeLa mitotic motor-induced movement was determined with an axoneme-based gliding assay (Pryer *et al.*, 1986). Growth of bovine brain tubulin onto the plus and minus ends of the axonemes was carried out (without taxol) at a tubulin concentration of 10 μM, which resulted in the formation of microtubules which were longer at the plus ends of axonemes and much shorter at the minus ends of axonemes. When D-100 fractions of HeLa mitotic cells were added to coverslips followed by addition of the axoneme constructs, the axonemes glided with their plus ends leading, i.e. minus end-directed movement (Figure 2). Plus end-directed motion was never observed.

To eliminate the possibility that the minus end-directed axoneme movement was due to axoneme-associated dynein, gliding assays were performed with the coverslips coated with bovine serum albumin instead of the D-100 fractions. No axonemes moved under these conditions (data not shown). To verify the direction of movement we constructed axonemes with microtubules at plus ends only using bovine brain tubulin treated with *N*-ethylmaleimide (NEM) (Hyman *et al.*, 1991) and again found that the axonemes moved with microtubule plus-ends leading (data not shown).

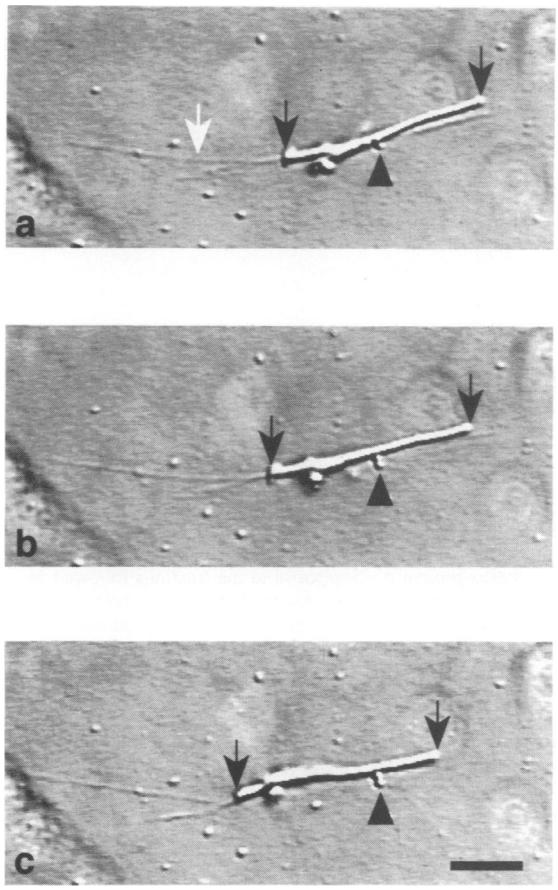

Fig. 2. Microtubule motility in mitotic HeLa cell extracts is minus-end directed. 1 μl volumes of a D-100 fraction were applied to coverslips and allowed to adsorb to the surface for 15–30 s. Microtubule–axoneme constructs prepared without taxol were then diluted into PEM_{50} buffer containing 20 μM tubulin, 2 mM GTP and 2 mM ATP, and 1 μl volumes of this mixture were added to the D-100 extract on the coverslips. (**a**)–(**c**) are video microscopy images taken at 5 s intervals at 25°C showing the movement of one such axoneme. The two ends of the axoneme are marked with dark arrows and a bovine brain microtubule at the axoneme plus end is marked with a white arrow. The dark arrowhead marks an object on the surface of the coverslip that did not move and serves as a reference point for movement of the axoneme. The axoneme moved with its plus end (long microtubules) leading. Movement of a total of 45 axoneme constructs with three different preparations of the D-100 fraction were evaluated. Only minus-end directed movement occurred. Bar = 3 μm.

The D-100 mitotic motor is associated with CENP-E

CENP-E has been postulated to be a microtubule motor based upon sequence similarity to the motor domain of kinesin (Yen *et al.*, 1991). Thus, we examined whether the motor activity present in the HeLa mitotic extracts might involve CENP-E by immunodepleting any CENP-E from the extracts. We used a polyclonal antiserum, HX-1, specific for the putative stalk domain of CENP-E (see Materials and methods). As shown in Figure 3, lanes 1 and 2, HX-1 quantitatively depleted CENP-E protein from the mitotic D-100 fractions. When the CENP-E-depleted D-100 fractions were examined for the ability to effect microtubule movement, no movement was detected (Figure 3, microtubule gliding motility is indicated for each supernatant fraction below the lane number; motility was quantitated as the reciprocal of the greatest dilution

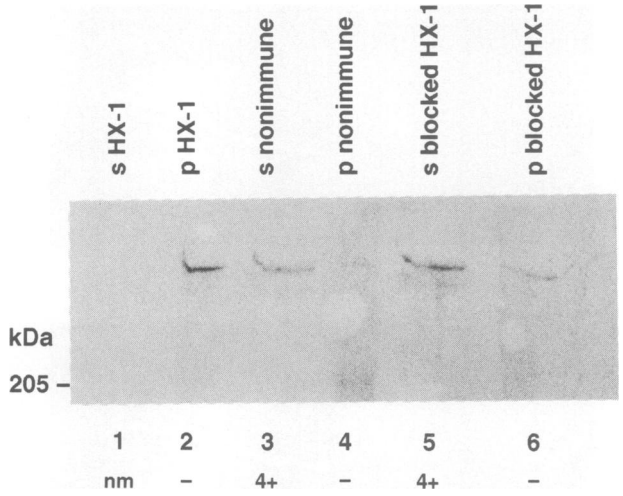

Fig. 3. Immunoprecipitation of CENP-E from D-100 fractions. D-100 fractions were immunoprecipitated by adding HX-1 antiserum and *Staphylococcus* protein A–Sepharose to the fractions followed by centrifugation (Materials and methods). The resulting pellets and supernatants were subjected to SDS–PAGE and immunoblotting with HX-1 antiserum. Microtubule gliding was assayed in the supernatants and the motility is shown for each lane below the lane number. Fractions with 4+ motility were active at a 4-fold dilution (Porter *et al.*, 1987), as was the D-100 extract prior to immunoprecipitation (not shown). nm, no motility. Fractions designated (–) were not assayed for motility. s HX-1 (lane 1), supernatant from the HX-1 immunoprecipitation; p HX-1 (lane 2), pellet from the HX-1 immunoprecipitation; s non-immune (lane 3), supernatant from the non-immune serum immunoprecipitation; p non-immune (lane 4), pellet from the non-immune serum immunoprecipitation; s blocked HX-1 (lane 5) supernatant from the HX-1 fusion protein-blocked HX-1 antibody; p blocked HX-1 (lane 6) pellet from the HX-1 fusion protein-blocked HX-1 antibody.

which supported motility). Non-immune control serum did not precipitate CENP-E protein from the mitotic D-100 fractions (Figure 3, lanes 3, 4), and did not remove any microtubule gliding activity. In addition, incubation of the HX-1 antiserum with the HX-1 fusion protein prior to adding the antiserum to the D-100 fractions prevented depletion of CENP-E (Figure 3, lane 5) and had no effect on the microtubule movement. These data indicate that the motor present in the HeLa mitotic D-100 fractions is associated with CENP-E.

Characterization of the CENP-E-associated motor

Nucleotide specificity. Previous studies have shown that different molecular motors have distinct pharmacological 'fingerprints' (Shimizu *et al.*, 1991). We characterized the motility of the CENP-E-associated motor in D-100 mitotic extracts with various nucleotide substrates to determine how the motor activity compared with the activities of kinesin and dynein. We found that the nucleotide specificity of the CENP-E-associated motor was different from that of either dynein or kinesin (Table I). For example, adenosine 5′-*O*-(3-thiotriphosphate) (ATPγS), which facilitates movement with dynein, did not promote movement with the CENP-E-associated motor (Table I). In contrast to kinesin (Shimizu *et al.*, 1991), neither GTP, 8-bromo ATP nor 1,N^6-etheno-adenosine 5′-triphosphate (etheno ATP) promoted movement with the CENP-E-associated motor (Table I).

Inhibitor specificity. Known inhibitors of kinesin and dynein motor activities were also used to examine the similarities and differences between the CENP-E-associated motor and kinesin and dynein. The pattern of inhibition of the CENP-E-associated motor activity was different from that previously reported for kinesin or dynein. In contrast to kinesin, yet similar to dynein (Vale and Toyoshima, 1989), the activity of the CENP-E-associated motor was completely inhibited by 10 μM sodium orthovanadate (Table II). In contrast to dynein but similar to kinesin, the activity of the CENP-E-associated motor was completely inhibited by 1 mM 5′-adenylylimidodiphosphate (AMP-PNP), and was not inhibited by 1 mM NEM or 1 mM erythro-9-[3-(2-hydroxynonyl)] adenine (EHNA) (Table II). We also found that 1 mM AMP-PNP induced a rigor state with the CENP-E-associated motor that was similar to that produced with kinesin (Porter *et al.*, 1987) in which microtubules became bound to the surface of the coverslips. In contrast, high concentrations of AMP-PNP promote release of the microtubules from dynein-coated coverslips (Mitchell and Warner, 1981). Thus the pattern of inhibition of the CENP-E-associated motor activity is distinct from that of dynein or kinesin.

Conditions that inactivate or block dynein motility do not affect the CENP-E-associated motility in mitotic D-100 fractions

Based upon the foregoing results, the mitotic motor activity present in the HeLa mitotic extracts did not appear to be due to dynein. However, because the motor activity was minus-end directed and because dynein-like motors have been detected in extracts of cultured chick embryo fibroblasts and sea urchin eggs (Schroer *et al.*, 1989; Gliksman and Salmon, 1993), we used two different strategies to eliminate the possibility that a form of dynein was responsible for the gliding activity in the HeLa mitotic extracts.

Dynein is inactivated by vanadate–UV-photocleavage of the dynein heavy chain (Gibbons *et al.*,1987). Thus, in the first strategy, we determined whether photo-inactivation of any possible dynein in the D-100 fraction could destroy or alter gliding motility. Under the conditions used, exposure of purified HeLa dynein to UV irradiation in the presence of sodium orthovanadate cleaved the dynein into two fragments as expected (data not shown). Dynein that was not photo-inactivated supported microtubule gliding (Figure 4B) whereas no microtubule gliding was observed with HeLa dynein that had been UV irradiated in the presence of orthovanadate (Figure 4A). In contrast, microtubule motor activity in D-100 extracts was unchanged following incubation with orthovanadate and UV irradiation (Figure 4C and E).

Antibodies to dynein are available that are capable of blocking dynein-mediated microtubule motility (Vaisberg *et al.*, 1993). Thus in a second strategy, we used an antibody to the phosphate binding loop of *Dictyostelium* dynein (Bob), to determine whether the microtubule gliding activity in the D-100 fractions could be blocked by the antibody (Figure 4). Addition of the anti-dynein antibody Bob to the D-100 fraction had no effect on microtubule gliding (Figure 4, compare E with C). In contrast, the Bob antibody completely blocked dynein-mediated microtubule gliding (Figure 4, compare F with

Table I. Nucleotide dependence of the CENP-E-associated motor

Nucleotide	CENP-E-associated motor[a]		Kinesin[b]		Dynein[b]	
	Rate[c]	%[d]	Rate[c]	%[d]	Rate	%[d]
ATP	0.24 ± 0.02	100	0.42 ± 0.06	100	4.5 ± 1.0	100
GTP	0	0	0.11 ± 0.06	27	0	0
2'dATP	0.21 ± 0.02	88	0.38 ± 0.07	91	1.3 ± 0.3	28
3'dATP	0.20 ± 0.02	83	0.30 ± 0.06	72	2.0 ± 0.5	44
ddATP	0.15 ± 0.01	62	0.29 ± 0.05	69	0.9 ± 0.3	21
8-Bromo ATP	0	0	0.01 ± 0.01	3	0	0
8-Azido ATP	0	0	0	0	0	0
Etheno ATP	0	0	0.05 ±0.03	13	0	0
ATPγS	0	0	0.01 ± 0.01	2.2	0.21 ± 0.1	4.6

[a]CENP-E-associated motor gliding rates were measured at 25°C as described in Materials and methods. Rates are mean and standard deviation.
[b]Kinesin and *Tetrahymena* 22S ciliary dynein rates (μm/s) determined by Shimizu *et al.* (1991). Kinesin rates were measured at 22–24°C and dynein rates at 25°C.
[c]Rates are the mean and standard deviation in μm/s from three different mitotic D-100 fractions; a total of 45 microtubules were analyzed for each condition.
[d]Percent of the rate of movement induced by 1 mM ATP.

Table II. Effects of microtubule motor inhibitors on the rate of CENP-E-associated motor-induced movements

Inhibitor	Rates of microtubule gliding (as % untreated control)		
	CENP-E-associated motor[a]	Kinesin[b]	Dynein[b]
AMP-PNP (1 mM)	0	0	100
Vanadate (10 μM)	0	100	0
NEM (1 mM)	98	94	0
EHNA (1 mM)	96	104	35

[a]CENP-E motor rates were obtained as described in Materials and methods. Gliding motility was assayed in three different D-100 mitotic extracts; a total of 45 microtubules were analyzed for each condition.
[b]Data of Vale and Toyoshima (1989).

B). A non-immune serum control did not block dynein-mediated motor activity (data not shown). Thus, we can conclude that the CENP-E-associated motility in the HeLa mitotic D-100 fractions was not due to dynein.

Further purification and characterization of CENP-E-associated motor activity

Microtubule-affinity purification. CENP-E has been shown to bind to microtubules in an ATP-sensitive manner (Yen *et al.*, 1992). Thus, the affinity of CENP-E for bovine brain microtubules and its release with 10 mM Mg^{2+}ATP and 0.5 M NaCl was used to further purify the CENP-E-associated motor from mitotic D-100 fractions (Materials and methods). D-100 mitotic fractions were incubated with microtubules and the microtubules with bound motor activity were sedimented through sucrose cushions and washed in PEM_{100} buffer to remove non-microtubule-bound proteins. The CENP-E bound quantitatively to the microtubules and the CENP-E was mostly depleted from the D-100 supernatant after sedimentation of the microtubules (data not shown). Motor activity could not be eluted with PEM_{100} buffer but was readily eluted from the microtubules with PEM buffer containing 10 mM Mg^{2+}ATP and 0.5 M NaCl. Approximately 70% of the CENP-E that was originally bound to microtubules was

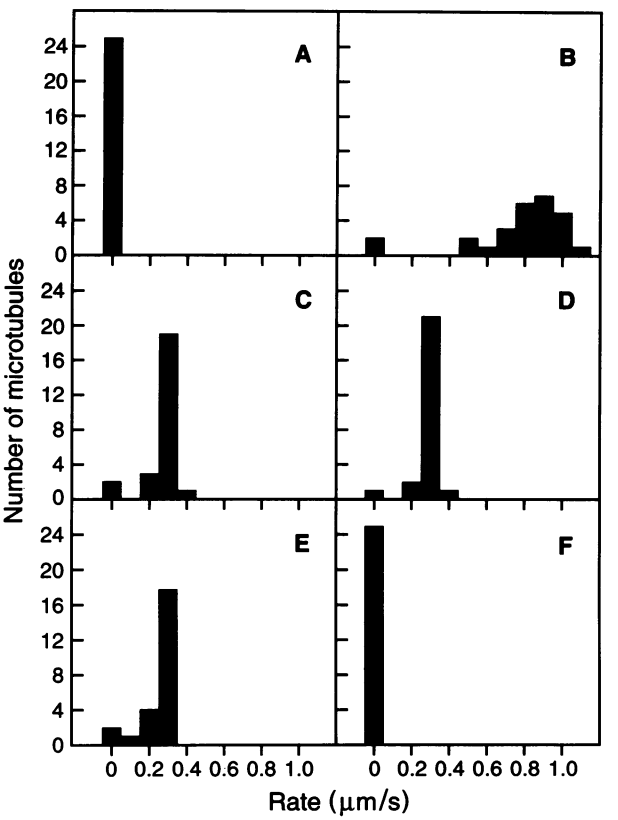

Fig. 4. Comparison of microtubule gliding induced by CENP-E containing D-100 fractions or by purified HeLa cell dynein before and after inactivation of dynein. Dynein-based motility was inactivated by UV irradiation in the presence of sodium orthovanadate (**A**) or by incubation with a dynein motility-blocking antibody, Bob (**F**). Untreated dynein (**B**), UV−vanadate-treated dynein (A), Untreated D-100 fraction (**C**), UV−vanadate treated D-100 fraction (**D**). D-100 fraction (**E**) and dynein (F) incubated with a dynein motility-blocking antibody. UV−vanadate treatment inhibited motility of dynein (compare B with A) but did not inhibit motility of D-100 fractions (compare D with C). The dynein antibody Bob blocked dynein induced motility (compare F with B) but not that of D-100 extracts (compare E with C).

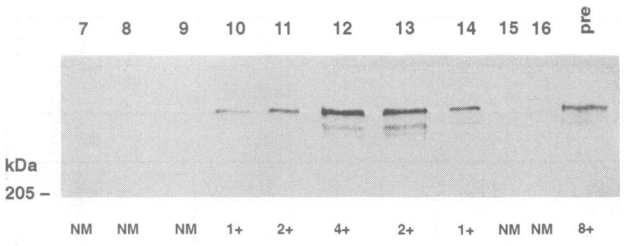

Fig. 5. Sucrose density centrifugation of microtubule affinity-purified CENP-E-associated motor activity. CENP-E-associated motor activity was eluted from microtubules with a solution of 10 mM Mg^{2+}ATP, 0.5 M NaCl, in PEM_{100} buffer. Eluted proteins were centrifuged through a 5–20% sucrose gradient. Thirty-five 2-drop fractions were collected from the bottom of the tube. Duplicate 20 µl samples of sucrose gradient fractions 7–13 were subjected to SDS–PAGE and immunoblotted with HX-1 antibody. A 5 µl sample of the ATP/NaCl microtubule-eluted fraction was loaded into the final lane (labeled pre). All 35 gradient fractions were assayed for microtubule gliding; gliding activity is indicated below each fraction as described in Figure 3. NM, no motility.

extracted with 10 mM Mg^{2+}ATP and 0.5 M NaCl. Extraction with 10 mM Mg^{2+}ATP and 0.5 M NaCl was routinely used to obtain CENP-E-associated motor activity in subsequent purification steps. The remaining NaCl-resistant fraction likely represents the phosphorylation-sensitive, NaCl-resistant fraction of CENP-E (Liao *et al.*, 1994).

Sucrose density gradient sedimentation of the CENP-E-associated motor. Further purification of the CENP-E-associated motor was accomplished by fractionating the ATP/NaCl-eluted motor through a 5–20% sucrose gradient. An immunoblot of the gradient fractions (Figure 5) showed that CENP-E appeared in fractions 10–14, the identical fractions that exhibited motor activity. Coincident with the highest level of CENP-E, fraction 12 also contained the most gliding activity. A protein band having the same molecular mass as CENP-E was visible on a silver-stained SDS–PAGE gel of fractions 10–14, and the quantity of the protein correlated well with the amount of CENP-E that was detected by immunoblotting (data not shown). A second CENP-E cross-reactive protein band that migrated on SDS–PAGE gels a little faster than the major band could be detected on immunoblots of CENP-E-containing fractions when the protein was loaded directly onto the SDS–PAGE gel without prior immunoprecipitation (see lanes 12, 13 and 14 in Figure 5). The nature of the second CENP-E band is not known.

The gliding activity in each of the peak sucrose density fractions was characterized and found to be indistinguishable from the gliding activity previously described in D-100 fractions of HeLa mitotic extracts. Specifically, the gliding activity was minus-end directed and occurred at a mean rate of 0.22 ± 0.03 µm/s (25°C). In addition, the pattern of response to motor inhibitors (AMP-PNP, sodium orthovanadate, NEM and EHNA) and to GTP as a nucleotide substrate was identical to that reported in Figure 2 for the CENP-E-associated motor in D-100 fractions. Thus, the motor activity displayed the same rate, directionality and inhibitor specificity of the activity described in the less purified preparation.

CENP-E from the peak gel fractions was also immunoprecipitated with HX-1 to verify that depletion of CENP-E

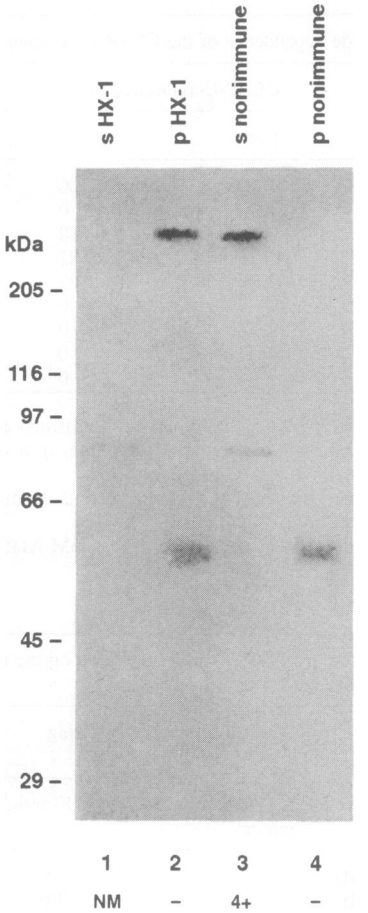

Fig. 6. Immunoprecipitation of sucrose gradient-purified CENP-E removed microtubule motor activity. Fractions 12 and 13 of the sucrose gradient (Figure 5) were pooled and immunoprecipitated with either HX-1 antibody or with non-immune serum. Pellet and supernatant fractions were subjected to SDS–PAGE and immunoblotted with HX-1. Supernatant after HX-1 immunoprecipitation (lane 1), pellet after HX-1 immunoprecipitation (lane 2), supernatant, non-immune serum control (lane 3), pellet, non-immune serum control (lane 4). Supernatants were assayed for motility as described in Figure 3. NM, no motility.

removed the motor activity. As shown in Figure 6, lanes 1 and 2, CENP-E was immunodepleted by HX-1 from pooled sucrose gradient fractions 12 and 13, and CENP-E appeared in the resulting pellet (p HX-1). The use of non-immune serum did not result in depletion of CENP-E (lanes 3 and 4). Immunodepletion of CENP-E resulted in the complete loss of microtubule gliding activity (Figure 6, lane 1).

Physical characteristics of the CENP-E-associated motor. The native molecular weight and axial ratio of the CENP-E-associated motor was estimated from sucrose density sedimentation and gel filtration data (data not shown). The motor activity co-migrated with CENP-E protein by gel filtration on Sepharose 4B 200, and a diffusion coefficient of 1.27 ± 0.04 × 10^7 cm^2/s was determined for the CENP-E-associated motor using standards of known diffusion coefficients (Bloom *et al.*, 1988). CENP-E-associated motor that had been extracted from microtubules with ATP/NaCl as described above was subjected to sucrose gradient sedimentation along with standards of known sedimentation coefficients (Materials

and methods). Three different determinations yielded a sedimentation coefficient for the CENP-E-associated motor of 12.6 ± 0.7 × 10^{-13} s. A native molecular weight for the CENP-E-associated motor of 874 000 ± 156 000 Da was calculated from the Svedberg equation assuming a partial specific volume of 0.725 ± 0.020 cm^3/g, a Stokes' radius of 16.9 ± 0.6 nm was calculated from the diffusion coefficient, and a frictional coefficient of 2.63 was derived from the molecular weight and Stokes' radius. We made the assumption that the overall shape of the CENP-E-associated motor, like kinesin (Bloom *et al.*, 1988), is approximated by a prolate ellipsoid, and calculated the axial ratio to be 40:1. Based on the foregoing parameters, the CENP-E-associated motor can be estimated to have dimensions of 2 nm × 80 nm.

Discussion

We have found that extracts of HeLa cells blocked in mitosis with vinblastine contain a minus-end directed microtubule motor activity that was not detected in extracts of interphase cells. Removal of CENP-E protein from the extracts with an antibody specific for CENP-E eliminated all microtubule gliding activity. CENP-E-associated motor activity was distinct from the activities of dynein and kinesin based upon microtubule gliding rates and nucleotide specificity and inhibitor specificity. Finally, the CENP-E motor activity co-purified with CENP-E protein in several purification steps.

Is the minus-end directed mitotic HeLa cell motor CENP-E?

Based on the evidence described in this work, we think that the minus-end directed motor present in mitotic HeLa extracts may be CENP-E itself. First, CENP-E is predicted to be a microtubule motor because a region near its N-terminus has a kinesin-like motor domain sequence that binds to microtubules in an ATP-sensitive manner (Yen *et al.*, 1992; Liao *et al.*, 1994). Second, the motor activity was removed from the mitotic D-100 fraction and from sucrose gradient fractions by immunoprecipitation with an antibody specific for CENP-E (Figures 3 and 6). Third, CENP-E protein co-fractionated with the motor activity in all purification steps, which included microtubule-affinity, gel filtration and sucrose density gradient centrifugation steps. Fourth, the motor activity was not due to dynein (also a minus-end directed motor) or to kinesin (Tables I and II). For example, blocking of dynein-mediated motor activity with a dynein-specific antibody had no effect on the CENP-E-associated motor activity (Figure 4). However, while it does not seem very likely, the present data do not formally exclude the possibility that the CENP-E-associated minus-end directed motor is due to an undetected protein that binds tightly to CENP-E. Such a protein might be a functional part of a CENP-E complex, or it could associate with CENP-E fortuitously.

Characterization of the CENP-E-associated motor

Rates of movement. The CENP-E-associated motor moved microtubules more slowly than kinesin, dynein or the KLP KIF3A, but somewhat faster than other KLPs such as Eg5, Kar3 and ncd. The CENP-E-associated motor moved microtubules at a mean rate of 0.46 μm/s at 37°C and 0.24 μm/s at 25°C, while the reported rates for microtubule movement with kinesin are 0.4–0.9 μm/s at 22–25°C (Vale *et al.*, 1985; Porter *et al.*, 1987; Saxton *et al.*, 1988) and the reported rates for HeLa cell dynein-mediated microtubule gliding are 4 μm/s at 37°C and 1.5 μm/s at 24°C (Lye *et al.*, 1989). (We obtained gliding rates of 0.9 μm/s with HeLa dynein at 25°C, see Figure 4A.) CENP-E-associated microtubule gliding was more rapid than gliding effected by the KLPs Eg5 (0.04 μm/s; Sawin *et al.*, 1992), ncd (0.07–0.12 μm/s; McDonald *et al.*, 1990; Walker *et al.*, 1990) and Kar3 (0.02–0.03 μm/s; Endow *et al.*, 1994), but slower than gliding effected by KIF3A (0.6 μm/s; Kondo *et al.*, 1994).

Direction of movement. In view of the fact that the motor domain of CENP-E is located at its N-terminus and that kinesin and other plus-end directed KLPs have their motor domains at the N-termini (Nislow *et al.*, 1992; Sawin *et al.*, 1992; Goldstein, 1993), it is curious that the CENP-E-associated motor isolated from prometaphase/metaphase HeLa cell extracts is minus-end directed (Figure 2). The KLPs that have been shown previously to be minus-end directed are ncd (McDonald *et al.*, 1990; Walker *et al.*, 1990) and Kar3 (Endow *et al.*, 1994), whose motor domains are at their C-termini. Such data have given rise to a model in which plus-end directed kinesin-like motors would have N-terminal motor domains and minus-end directed kinesin-like motors would have C-terminal motor domains. However, Stewart *et al.* (1993) found that chimeric proteins containing a C-terminal kinesin motor domain or an N-terminal ncd motor domain maintained their original directionality, demonstrating that the location of the motor domain in the primary protein sequence of ncd and kinesin does not determine the direction of movement. If CENP-E is responsible for the activity described here, it is the first naturally occurring minus end-directed motor whose motor domain is at its N-terminus.

Nucleotide and inhibitor specificities of the CENP-E-associated motor. The nucleotide and inhibitor specificities of the CENP-E-associated motor were distinct from other known motors. In particular, the nucleotide specificity for movement of CENP-E and kinesin were significantly different (Table I), indicating that kinesin-like motor domains do not necessarily have similar nucleotide specificities. Three out of four motor-inhibitory compounds likewise gave results that contrasted with those reported with dynein (Table II). The nucleotide specificity for the CENP-E-associated motor was also different from that of a Kar3 fusion protein (Endow *et al.*, 1994), KIF3A (Kondo *et al.*, 1994) and the kinetochore-associated motor activities described by Hyman and Mitchison (1991).

Physical characteristics of CENP-E and its associated motor activity. The native molecular weight of CENP-E was estimated to be ~874 000 Da as determined for bovine brain kinesin, assuming a partial specific volume for CENP-E of 0.725 ± 0.020 cm^3/g (Bloom *et al.*, 1988). Based upon its predicted amino acid sequence (Yen *et al.*, 1992) CENP-E itself would be expected to have a molecular weight of 312 000 Da. Other molecular motors including myosin, kinesin and dynein are complexes composed of one or two heavy chains and a number of

low-molecular-weight proteins. Similarly, CENP-E may be a dimer and/or it may complex with other proteins.

The calculated molecular dimensions of the native CENP-E-associated motor suggest that it is a long, rod-shaped structure (2 nm × 80 nm) which is twice the estimated length of kinesin (Bloom *et al.*, 1988). Because the amino acid sequence of the putative stalk domain of CENP-E is nearly four times longer than that of kinesin, it is possible that the putative stalk region is not as extended as the stalk region of kinesin. Alternatively, there are several interruptions of the predicted α-helical sequence of the stalk region of CENP-E (Yen *et al.*, 1992) which may create 'hinge regions' such as the bent region of the kinesin molecule which has been visualized by electron microscopy (Hisanaga *et al.*, 1989).

Possible mitotic functions of the CENP-E-associated motor. Microtubule motors are important for chromosome movements and spindle organization during mitosis (McIntosh, 1994). For example, mutations in the gene coding for ncd (Endow *et al.*, 1990) or for cytoplasmic dynein (Li *et al.*, 1993) yielded abnormal mitotic phenotypes. In addition, injection of antibodies to dynein or to the motor domain of kinesin blocked spindle pole separation in PtK_1 cells (Rodionov *et al.*, 1993; Vaisberg *et al.*, 1993) and injection of an antibody to the MKLP-1 motor prevented the PtK_1 cells from transitioning into anaphase (Nislow *et al.*, 1990). Also, microtubules attached to kinetochores of chromosomes *in vitro* can move relative to the kinetochores either in a plus-end directed or minus-end directed manner, indicating that kinetochores contain functional microtubule motors (Hyman and Mitchison, 1991).

The rate of rapid poleward movement of chromosomes that occurs soon after the capture of microtubules by kinetochores during prometaphase (Hayden *et al.*, 1990; Rieder and Alexander, 1990) has been reported to be 0.38 μm/s in PtK_1 cells at 37°C (Roos, 1976), and 0.13 μm/s 23–24°C (Merdes and De Mey, 1990). These rates are similar to the rates of microtubule gliding observed in the present study with the CENP-E-associated motor (0.46 μm/s at 37°C and 0.24 μm/s at 25°C). Because CENP-E is first detected at kinetochores at prometaphase, it is conceivable that CENP-E may participate in rapid poleward movement of chromosomes during prometaphase. In addition, because CENP-E remains at the kinetochores through metaphase, its motor activity may contribute to the oscillations (Skibbens and Skeen, 1993) of chromosomes as they congress toward the metaphase plate.

Materials and methods

Cell culture, S-100 extracts and D-100 fractions of mitotic and interphase cells

HeLa S3 cells (American Type Culture Collection) were grown in spinner cultures at 37°C in BioRich-1 medium (ICN, Irvine, CA) supplemented with modified Eagle's medium non-essential amino acids, penicillin (5000 U/ml), streptomycin (5 mg/ml), 10 mM HEPES buffer (Fisher, Los Angeles, CA), 1.5 g/l glucose and 2% calf serum. Mitotic cells were obtained by growing cells to a density of 4–6 × 10^5 cells/ml followed by incubation with 2–5 nM vinblastine sulfate for one cell cycle (22–24 h). Most (90–95%) of the cells were blocked in mitosis (Jordan *et al.*, 1991). Interphase cells were obtained from an exponentially growing cell culture; 96% of the cells were in interphase and 4% were in mitosis.

Cells were separated from the culture media by centrifugation. Cell pellets were washed by resuspension and sedimentation in phosphate-buffered saline and then in 50 mM piperazine-*N*, *N*′-bis-(2-ethanesulfonic acid), 1 mM EGTA, 1 mM $MgSO_4$, 0.05% sodium azide (PEM_{50} buffer). Cell pellets were resuspended in equal volumes of PEM_{50} buffer containing 1 mM tosyl arginine methyl ester, 10 μg/ml aprotinin, 1 μg/ml leupeptin, 2.5 μg/ml 4-(2-aminoethyl)-benzenesulfonyl fluoride and 1 mM dithiothreitol (PEM_{50}/PID), and lysed by sonication at 0°C followed by incubation at 0°C for 20 min to ensure complete microtubule depolymerization. The lysate was centrifuged (100 000 *g*, 4°C, 30 min) and the resulting supernatant solution, which contained the HeLa mitotic motor activity, was called the S-100 extract. The S-100 extract could be stored frozen at −70°C for at least 4 months without loss of motor activity.

Fractionation of the S-100 extract by DEAE−cellulose (DE52, Whatman, Maidstone, UK) column chromatography yielded a soluble protein fraction (the D-100 fraction). The D-100 fraction was prepared by incubating the S-100 extract with an equal volume of DEAE−Sepharose for 40 min at 4°C, pouring the mixture into a 2.5 cm × 20 cm column, and eluting the column with PEM_{50}/PID buffer. The flow-through solution was concentrated to the volume of the original cell pellet with a Centriprep 30 centrifugal concentrator (Amicon, Beverly, MA) to form the D-100 fraction and frozen for later use in experiments or for further purification of mitotic motor activity.

Microtubule motor assays

A gliding assay in which microtubules move across the surface of glass coverslips (Vale *et al.*, 1985) was used to characterize the movement of the HeLa cell mitotic motor. Taxol-stabilized microtubules in 100 mM piperazine-*N*,*N*′-bis-(2-ethanesulfonic acid), 1 mM EGTA, 1 mM $MgSO_4$, 0.05 % sodium azide (PEM_{100} buffer) and 10 μM taxol (National Cancer Institute) were diluted for use in motility assays to a tubulin concentration (in microtubules) of 0.1 μM. ATP or other nucleotides were added as appropriate. A 1 μl volume of protein fraction to be assayed for motor activity was placed on a 12 mm diameter glass coverslip and incubated at room temperature for 15–30 s. A 1 μl volume of the taxol-stabilized microtubule suspension was then added and the 12 mm coverslip was sandwiched between an 18 mm diameter coverslip and a pre-warmed microscope slide (Toso *et al.*, 1993). Microtubule images were captured by video-enhanced differential interference microscopy on a Zeiss IM-35 microscope with a temperature-controlled stage using a Hamamatsu C2400 (Newvicon) video camera (Toso *et al.*, 1993). Rates of microtubule movement were determined with Real Time Measurement software (generously provided by Dr N.Gliksman, Duke University Medical Center, NC and Dr E.Salmon, University of North Carolina) used with a Video Van Gogh image analysis card (Tekmatic Systems, Ben Lomond, CA). Gliding activity was scored as the reciprocal of the greatest dilution that supported directional microtubule movement as described in Porter *et al.* (1987).

The direction of microtubule gliding was determined by an axoneme gliding assay (Pryer *et al.*, 1986). Axonemes from *Strongylocentrotus purpuratus* and axoneme−microtubule constructs were prepared as described by Toso *et al.* (1993) except that a tubulin concentration of 10 μM was chosen to promote microtubule growth primarily at plus ends of axonemes. Tubulin was added to the gliding assay at a final concentration of 10 μM to prevent dilution-induced depolymerization of microtubules which could result in an incorrect assignment of polarity to axonemes. Some assays were carried out with axoneme−microtubule constructs formed with NEM-treated tubulin (Hyman *et al.*, 1991) mixed in equal proportion with untreated tubulin (final tubulin concentration, 20 μM) to prevent microtubule polymerization at minus ends of the axonemes.

Dynein antibody motility blocking assays (Vaisberg *et al.*, 1993) were performed by adsorbing dynein or D-100 fractions onto coverslips for 15 min and 30 s, respectively. Affinity-purified rabbit antiserum to *Dictyostelium* dynein (Bob) (a generous gift from Dr E.Vaisberg, University of Colorado, Boulder, CO) (0.6 mg/ml), or non-immune serum was added to coverslips and incubated for 15 min prior to the addition of microtubules and ATP.

Nucleotide specificity

Rates of microtubule movement were determined in the presence of 1 mM nucleotide; nucleotides were from Sigma, St Louis, MO. Commercially available analogs of ATP have been reported to be contaminated with as much as 1% ATP (Shimizu *et al.*, 1991). To control for the possibility that contaminating ATP might be responsible for observed microtubule motility with analogs, we incubated the ATP analogs with an ATP-depleting solution (see below) and repeated the gliding assays. With dideoxy ATP and the deoxy derivatives of ATP, the rates of microtubule

movement were unchanged by ATP depletion. However, a very slow rate of movement that had occurred initially with 8-azido ATP and with ATPγS was eliminated by depletion of ATP, indicating the presence of contaminating ATP in these two analog preparations.

Inactivation of dynein by the vanadate–UV photocleavage reaction

Samples of HeLa cell dynein (purified by the method of Pfarr *et al.*, 1990) or D-100 fractions were illuminated with a 365 nm light source at a distance of 2.5 cm in the presence of 10 μM sodium orthovanadate (Fisher) at 0°C for 50 min (Gibbons *et al.*, 1987). Samples were then incubated with a solution of 5 mM norepinephrine (Sigma) for 20 min at 0°C to inactivate the vanadate which otherwise would inhibit motility of dynein and the CENP-E-associated motor. Control samples were illuminated with UV light in the absence of vanadate. Treatment of control samples with norepinephrine did not affect gliding rates.

Antibody purification, immunoprecipitations and immunoblots

The generation and characterization of the antibody HX-1, a rabbit polyclonal antiserum raised to a fusion protein of a bacterially expressed segment of the putative CENP-E stalk region and which identifies a protein of size consistent with the predicted size of CENP-E on immunoblots of chromosomal proteins, is described in Yen *et al.* (1992), where it is referred to as pAb1. Antibody HX-1 was partially purified by ammonium sulfate fractionation and DEAE-adsorption prior to use in immunoprecipitation reactions (Harlow and Lane, 1988). Immunoprecipitation was performed by incubating a 1:200 dilution of the purified antisera with the sample (1 h, 0°C), followed by a similar incubation with an equal volume of *Staphylococcus* protein A–Sepharose and centrifugation to sediment the immunoprecipitated proteins. The supernatants were saved and the pellets washed extensively in PEM_{50} buffer to remove non-specifically bound proteins. Pellets were resuspended in an equal volume of SDS–PAGE sample buffer. Pellets and supernatants were subjected to SDS–PAGE (Laemmli, 1970). Gels were immunoblotted as described previously (Thrower *et al.*, 1991), with the following modifications; electrotransfers for CENP-E and dynein were carried out at 0.5 A for 2 h, HX-1 serum was used at a 1:500 dilution, and affinity-purified rabbit antiserum to *Dictyostelium* dynein (Bob) was used at 0.4 μg/ml.

Microtubule-affinity purification of the CENP-E-associated motor

A 40 ml sample of packed HeLa cells was processed as described above to obtain the D-100 fraction which was depleted of ATP by incubation with hexokinase (10 U/ml) and 50 mM glucose at 20°C for 30 min followed by centrifugation (100 000 *g*, 30 min, 10°C) to remove actomyosin. The pellet was discarded and taxol was added to the supernatant to a final concentration of 10 μM. Two-hundred μmoles of microtubule-associated protein-depleted bovine brain tubulin (Toso *et al.*, 1993) was polymerized in a separate tube by the addition of an equimolar concentration of taxol. The taxol-stabilized microtubules were then added to the supernatant from the previous step and incubated for 30 min at 4°C to allow HeLa cell proteins to bind to the microtubules. The microtubules were sedimented (4°C, 30 min, 100 000 *g*) through a 10 ml 20% sucrose cushion in PEM_{50}/PID buffer. The microtubules with adhering proteins were then resuspended in PEM_{100}/PID buffer containing 10 μM taxol and centrifuged (4°C, 10 min, 100 000 *g*, Beckman SW 50.1 rotor). Microtubule-binding proteins were dissociated from the microtubules by incubation with 400 μl of 10 mM $MgSO_4$, 10 mM ATP and 0.5 M NaCl, in PEM_{100}/PID buffer containing 10 μM taxol (1 h, 4°C) with centrifugation as in the previous step. Microtubule-binding proteins were further fractionated by centrifugation (14 h, 4°C, 200 000 *g*) through a 4 ml 5–20% sucrose gradient in PEM_{100} buffer.

Molecular weight and dimensions of the CENP-E-associated motor

The sedimentation coefficient of the CENP-E-associated motor was determined by sucrose density centrifugation with protein from three independent purifications. Protein standards were: cytochrome *c* (1.71S), bovine serum albumin (4.73S), rabbit IgG (7.05S), catalase (11.3S) and thyroglobulin (19.4S) (Sober, 1970). Assignment of a sedimentation coefficient for CENP-E was accomplished by plotting sedimentation coefficients of the standards as a function of their elution positions and comparing the elution position of CENP-E with the standards by linear regression analysis.

The diffusion coefficient, $D_{20,w}$, of CENP-E was measured by gel filtration with a 20 ml Sepharose 4B-200 (Pharmacia, Piscataway, NJ) column equilibrated in PEM_{100} and 10% (w/v) glycerol. Protein standards and their diffusion coefficients were: myosin (1.16), bovine lens α crystallin (2.00), *E.coli* β galactosidase (3.12), *Bacillus* urease (3.46), and β amylase (5.77) ($\times 10^7$ cm^2/s) (Sober, 1970). K_{av} values were calculated from the formula $K_{av} = (V_e - V_0)/(V_t - V_0)$. Mean K_{av} values of standards were plotted versus $1/D_{20,w}$ and the diffusion coefficient of CENP-E was calculated by linear regression analysis.

The native molecular weight, Stokes' radius, and axial ratio of CENP-E were derived from the sedimentation coefficient and diffusion coefficient as described for kinesin by Bloom *et al.* (1988). The partial specific volume, $\bar{\upsilon}$, was assumed to be 0.725 ± 0.020 cm^3/g (the mean of 13 globular and fibrous proteins commonly used as molecular weight standards; Tanford, 1961). The Stokes' radius was calculated from the diffusion coefficient (Bloom *et al.*, 1988). The axial ratio was derived from Table 12.1 of Freifelder (1982), using a frictional ratio, $f/f_0 = a \div (3\bar{\upsilon}\ M_r/4\pi N)^{1/3}$ with *a* equal to Stokes' radius and N equal to Avogadro's number (Siegel and Monty, 1966).

Acknowledgements

We thank Mr Herb Miller for the preparation of tubulin and Drs John Carbon and Kim Middleton for critical reading of the manuscript. These studies were supported by American Cancer Society Grant DHP-43F. T.J.Y. is a Lucille C.Markey Scholar supported by USPHS GM44762, CA06927 and the Markey Charitable Trust.

References

Allan,V.J. and Vale,R.D. (1991) *J. Cell Biol.*, **113**, 347–359.
Bloom,G.S., Wagner,K., Pfister,K. and Brady,S.T. (1988) *Biochemistry*, **27**, 3409–3416.
Brown,K.D., Coulson,T.J., Yen,T.J. and Cleveland,D. (1994) *J. Cell Biol.*, **125**, 1303–1312.
Endow,S.A., Henikoff,S. and Soler-Niedziela,L. (1990) *Nature*, **345**, 81–83.
Endow,S.A., Kang,S.J., Satterwhite,L.L., Rose,M.D., Skeen,V.P. and Salmon,E.D. (1994) *EMBO J.*, **13**, 2708–2713.
Freifelder,D. (1982) *Physical Biochemistry*. W.H.Freeman and Co., San Francisco, CA.
Gibbons,I.R., Lee-Eiford,A., Mocz,G., Phillipson,C.A., Tang,W.J.Y. and Gibbons,B.H. (1987) *J. Biol. Chem.*, **262**, 2780–2786.
Gliksman,N.R. and Salmon,E.D. (1993) *Cell Motil.*, **24**, 167–178.
Goldstein,L.S.B. (1993) *Annu. Rev. Genet.*, **27**, 319–351.
Harlow,E. and Lane,D. (1988) *Antibodies: A Laboratory Manual*. Cold Spring Harbor Laboratory Press, Cold Spring Harbor, NY.
Hayden, J.H., Bowser,S.S. and Rieder,C.C. (1990) *J. Cell Biol.*, **111**, 1039–1045.
Hisanaga,S., Hirtma,M., Okuhara,K., Sato,R., Masuda,Y., Sakai,H. (1989) *Cell Motil.*, **12**, 264–272.
Hyman,A.H. and Mitchison,T.J. (1991) *Nature*, **351**, 206–211.
Hyman,A., Dreschel,D., Kellogg,D., Salser,S., Sawin,K., Steffen,P., Wordeman,L. and Mitchison,T. (1991) *Methods Enzymol.*, **196**, 478–496.
Jordan,M.A., Thrower,D. and Wilson,L. (1991) *Cancer Res.*, **51**, 2212–2222.
Kondo,S., Sato-Yoshitake,R., Noda,Y., Aizawa,H., Nakata,T., Matsuura,Y. and Hirokawa,N. (1994) *J. Cell Biol.*, **125**, 1095–1107.
Laemmli,U.K. (1970) *Nature*, **27**, 680–685.
Li,Y., Yeh,E., Hays,T. and Bloom,K. (1993) *Proc. Natl Acad. Sci. USA*, **90**, 10096–10100.
Liao,H., Li.,G. and Yen,T. (1994) *Science*, **265**, 394–398.
Lye,R.J., Pfarr,C.M. and Porter,M.E. (1989) In Warner,F.D. and McIntosh,J.R. (eds), *Cell Movement*. Alan R.Liss Inc., New York, pp. 151–152.
McDonald,H.B., Stewart,R.J. and Goldstein,L.S.B. (1990) *Cell*, **63**, 1159–1165.
McIntosh,J.R. (1994) In Hyams,J.S. and Lloyd,C.W. (eds), *Microtubules*. Wiley–Liss, Inc., New York, pp. 413–434.
Merdes,A. and De Mey,J. (1990) *Eur. J. Cell Biol.*, **53**, 313–325.
Mitchell,D.R. and Warner,F.D. (1981) *J. Biol. Chem.*, **256**, 12535–12544.
Nislow,C., Sellitto,C., Kuriyama,R. and McIntosh,J.R. (1990) *J. Cell Biol.*, **111**, 511–522.
Nislow,C., Lombillo,V.A., Kuriyama,R. and McIntosh,J.R. (1992) *Nature*, **359**, 543–547.

Pfarr,C.M., Coue,M., Grissom,P.M., Hays,T.S., Porter,M.E. and McIntosh,J.R. (1990) *Nature*, **345**, 263–265.
Porter,M.E., Scholey,J.M., Stemple,D.L., Vigers,G.P.A., Vale,R.D., Sheetz,M.P. and McIntosh,J.R. (1987) *J. Biol. Chem.*, **262**, 2794–2802.
Pryer,N.K., Wadsworth,P. and Salmon,E.D. (1986) *Cell Motil.*, **6**, 537–548.
Rieder,C.L. and Alexander,S.P. (1990) *J. Cell Biol.*, **110**, 81–95.
Rodionov,V.I., Gelfand,V.I. and Borisy,G.G. (1993) *J. Cell Sci.*, **106**, 1179–1188.
Roos,U.-P. (1976) *Chromosoma*, **54**, 363–385.
Sawin,K.E., Mitchison,T.J. and Wordeman,L.G. (1992) *J. Cell Sci.*, **101**, 303–313.
Saxton,W.M., Porter,M.E., Cohn,S.A., Scholey,J.M., Raff,E.C. and McIntosh,J.R. (1988) *Proc. Natl Acad. Sci. USA*, **85**, 1109–1113.
Schroer,T.A., Steuer,E.R. and Sheetz,M. (1989) *Cell*, **56**, 937–946.
Shimizu,T., Furusawa,K., Ohashi,S., Toyoshima,Y.Y., Okuno,M., Malik,F. and Vale,R.D. (1991) *J. Cell Biol.*, **112**, 1189–1197.
Siegel,L.M. and Monty,K.J. (1966) *Biochim. Biophys. Acta*, **11**, 346–362.
Skibbens,R.V., Skeen,V.P. and Salmon,E.D. (1993) *J. Cell Biol.*, **122**, 859–875.
Sober,H.A. (ed.), (1970) *Handbook of Biochemistry.* CRC Press Cleveland, OH.
Stewart,R.J., Thaler,J.P. and Goldstein,L.S.B. (1993) *Proc. Natl Acad. Sci. USA*, **90**, 5209–5213.
Tanford,C. (1961) *Physical Chemistry of Macromolecules*. John Wiley and Sons, Inc., New York.
Thrower,D., Jordan,M.A. and Wilson,L. (1991) *J. Immunol. Methods*, **136**, 45–51.
Toso,R.J., Jordan,M.A., Farrell,K.W., Matsumoto,B. and Wilson,L. (1993) *Biochemistry*, **32**, 1285–1293.
Vaisberg,E.A., Koonce,M.P. and McIntosh,J.R. (1993) *J. Cell Biol.*, **123**, 849–858.
Vale,R.D., Reese,T.S. and Sheetz,M.P. (1985) *Cell*, **42**, 39–50.
Vale,R.D. and Toyoshima,Y.Y. (1989) In Warner,F.D. and McIntosh,J.R. (eds), *Cell Movement.* Alan R.Liss, Inc., Syracuse, NY, p. 293.
Walker,R.A., Salmon,E.D. and Endow,S.A. (1990) *Nature*, **347**, 780–782.
Yen,T.J., Compton,D.A., Wise,D., Zinkowski,R., Brinkley,B.R., Earnshaw,W.C. and Cleveland,D.W. (1991) *EMBO J.*, **10**, 1245–1254.
Yen,T.J., Li,G., Schaar,B.T., Szilak,I. and Cleveland,D.W. (1992) *Nature*, **359**, 536–539.

Received on September 30, 1994; revised on December 8, 1994